Title

CT–Guided Bone Biopsies in Metastatic Castration-Resistant Prostate Cancer: Factors Predictive of Maximum Tumor Yield

Journal

Journal of Vascular and Interventional Radiology, 28(8)

ISSN

1051-0443

Authors

Holmes, Michael G
Foss, Erik
Joseph, Gabby
et al.

Publication Date

2017-08-01

DOI

10.1016/j.jvir.2017.04.019

Peer reviewed

CLINICAL STUDY

CT–Guided Bone Biopsies in Metastatic Castration-Resistant Prostate Cancer: Factors Predictive of Maximum Tumor Yield

Michael G. Holmes, MD, Erik Foss, MD, Gabby Joseph, PhD, Adam Foye, BS, Brooke Beckett, MD, Daria Motamedi, MD, Jack Youngren, PhD, George V. Thomas, MD, Jiaoti Huang, MD, PhD, Rahul Aggarwal, MD, Joshi J. Alumkal, MD, Tomasz M. Beer, MD, Eric J. Small, MD, and Thomas M. Link, MD, PhD

ABSTRACT

Purpose: To evaluate the success rate of CT–guided bone biopsies in metastatic castration-resistant prostate cancer (mCRPC) and to investigate associated technical, imaging, and clinical parameters affecting diagnostic yields.

Materials and Methods: Eighty CT–guided bone biopsy specimens were obtained from 72 men (median age, 68 y; range, 49–89 y) enrolled in a multicenter trial to identify mechanisms of resistance in mCRPC. Successful biopsy was determined by histologic confirmation of tumor cells and successful isolation of RNA for molecular analysis.

Results: The overall success rate of CT–guided bone biopsies was 69% (55/80) based on histology and 64% (35/55) based on isolation of molecular material for RNA sequencing. Biopsies performed in lesions with areas of radiolucency had significantly higher diagnostic yields compared with lesions of predominantly dense sclerosis (95% vs 33%; $P = .002$) and lesions of predominantly subtle sclerosis (95% vs 65%; $P = .04$). Success rates increased in lesions with density $\leq$ 475 HU (79% for $\leq$ 475 HU vs 33% for $>$ 475 HU; $P = .001$) and in lesions with ill-defined margins (76% for ill-defined margins vs 36% for well-circumscribed margins; $P = .005$). Alkaline phosphatase was the only clinical parameter to correlate significantly with diagnostic yield (83% for $>$ 110 U/L vs 50% for $\leq$ 110 U/L; $P = .001$).

Conclusions: Image-guided bone tumor biopsies can be successfully used to acquire cellular and molecular material for analyses in patients with osteoblastic prostate cancer metastases. Diagnostic yields are significantly increased in lesions with areas of radiolucency, density $\leq$ 475 HU, ill-defined margins, and interval growth and in patients with alkaline phosphatase $>$ 110 U/L.

ABBREVIATIONS

mCRPC = metastatic castrate-resistant prostate cancer, PSA = prostate-specific antigen

Despite treatment advances over the last few decades, prostate cancer remains the second leading cause of death in men in the United States (1). Prostate cancer is a heterogeneous disease with variable clinical outcomes ranging from a well-differentiated microscopic tumor with little clinical significance to an aggressive, high-grade cancer resulting in widespread metastases and death (2,3). Poor clinical outcomes in patients with prostate cancer are most often associated with the development of resistance to conventional hormone deprivation therapy or so-called metastatic castrate-resistant prostate cancer (mCRPC) (4,5).

From the Departments of Radiology and Biomedical Imaging (M.G.H., G.J., D.M., T.M.L.) and Medicine (A.F., J.Y., R.A., E.J.S.) and UCSF Helen Diller Family Comprehensive Cancer Center (A.F., J.Y., R.A., E.J.S.), University of California, San Francisco, 513 Parnassus Avenue, S-261, San Francisco, CA 94143-0628; Departments of Diagnostic Radiology (E.F., B.B.), Medicine (J.J.A., T.M.B.), and Pathology (G.V.T.) and OHSU Knight Cancer Institute (J.J.A., T.M.B., G.V.T.), Oregon Health & Science University, Portland, Oregon; and Department of Pathology (J.H.), Duke University School of Medicine, Durham, North Carolina. Received December 19, 2016; final revision received April 10, 2017; accepted April 21, 2017. **Address correspondence to** M.G.H.; E-mail: Michael.Holmes@ucsf.edu

None of the authors have identified a conflict of interest.

Appendix A is available online at *www.jvir.org*.

J Vasc Interv Radiol 2017; ■:1–9

http://dx.doi.org/10.1016/j.jvir.2017.04.019

Bone tumor biopsies have become increasingly important for molecular analyses and treatment planning in patients with mCRPC. Absence of viable tumor cells and mutational differences between primary and metastatic lesions often preclude sampling from the prostate (2,3). The predominant source of tissue in most patients is from osteoblastic bone lesions with viable tumor trapped in a densely packed sclerotic matrix (6). Consequently, bone biopsies are technically challenging and often result in inadequate sample size or poor-quality material (7–9).

Current literature describing tissue acquisition in metastatic prostate cancer is limited. Reported success rates are 26%–77% depending on whether biopsies were performed with or without computed tomography (CT) guidance (10–12). Most reports in the literature describe diagnostic yield in terms of histologic confirmation of tumor cells (10,11); however, in clinical practice, successful extraction of molecular material is an increasingly important goal of these biopsy procedures. To our knowledge, only 1 other study has reported on image-guided bone biopsies in metastatic prostate cancer in terms of both histologic confirmation of tumor cells and successful isolation of molecular material. In a study of 54 biopsies, Spritzer et al (12) reported a 67% success rate based on histologic confirmation but a significantly lower 40% success rate based on successful RNA isolation.

Although prostate cancer biopsies are increasing in importance for personalized treatment, there are significant challenges to harvest sufficient material. The purpose of this study was to determine the frequency with which CT-guided bone biopsies in patients with mCRPC yielded adequate material for both histologic and RNA-based analyses in a large, prospective, multi-institutional study. A second objective was to investigate the technical, imaging, and clinical parameters driving the diagnostic yield.

MATERIALS AND METHODS

The biopsies analyzed in this study were performed between March 2013 and December 2015 as part of a prospective, single-cohort, observational phase II trial to identify adaptive mechanisms of resistance in mCRPC (ClinicalTrials.gov Identifier NCT02432001). The trial enrolled 300 men with mCRPC at 6 academic centers. Institutional review board approval was obtained from all participating centers. The primary endpoint was to identify the proportion of patients with mCRPC with high androgen receptor activity in bone following second-line hormonal therapy and/or chemotherapy. For the present study, biopsies from 2 of the centers with the highest numbers of bone biopsies were analyzed.

Patients

The present study included 72 men (median age, 68 y; range, 49–89 y) who underwent 80 bone biopsies (8 patients had a second biopsy of a different lesion at the time of disease progression). Baseline clinical characteristics of the patients are presented in **Table 1**. The inclusion criteria consisted of (*a*) histologically confirmed prostate cancer, (*b*) radiographic evidence of metastatic disease amenable to image-guided biopsy (CT and bone scintigraphy), and (*c*) disease progression despite castrate levels of testosterone (< 50 ng/dL). The criteria for disease progression are described in **Appendix A** (available online at *www.jvir.org*) (13). All patients provided informed consent before undergoing biopsy.

Table 1. Baseline Patient Characteristics

Characteristics	Number of Biopsies (n = 80)	Median (q1–q3) or Percent
Age, y	80	68 (64–74)
Race		
White	64	81%
Other	3	16%
Unknown	13	4%
Gleason score		
≥ 8	59	74%
7	25	31%
≤ 6	6	8%
PSA, μg/L	80	45 (16–162)
Alkaline phosphatase, U/L	77	116 (72–275)
Hemoglobin, g/dL	75	12.5 (11.1–13.4)
Lactate dehydrogenase, U/L	49	204 (168–255)
Extent of metastatic disease		
Pelvis only	8	10%
Entire skeleton	72	90%
Androgen deprivation therapy	80	100%
Systemic chemo-/immunotherapy*	10	25%
Bone-modifying agent†	38	48%
External-beam radiation‡	20	26%

PSA = prostate specific antigen; q1 = first quartile; q3 = third quartile.
*Subset of population (n = 40).
†Zoledronate (n = 8); denosumab (n = 30).
‡Subset of population (n = 76).

Clinical and Laboratory Data

Clinical and laboratory data were analyzed based on review of the medical records. The following laboratory parameters were assessed as continuous variables: (*i*) hemoglobin (g/dL), (*ii*) prostate-specific antigen (PSA) (ng/mL), (*iii*) serum alkaline phosphatase (U/L), and (*iv*) lactate dehydrogenase (U/L). Laboratory values collected ± 30 days from the time of biopsy were considered relevant for the purposes of the analysis. The following data were collected and assessed as categorical variables: (*i*) bone-modifying agents (ongoing treatment > 6 months before biopsy) including the specific agent (zoledronate or denosumab) and the length of therapy (≤ 12 months vs > 12 months), (*ii*) systemic immunotherapy or chemotherapy (treatment at any point < 6 months before biopsy), (*iii*) androgen deprivation therapy (ongoing treatment > 6 months before biopsy), and (*iv*) external-beam radiation

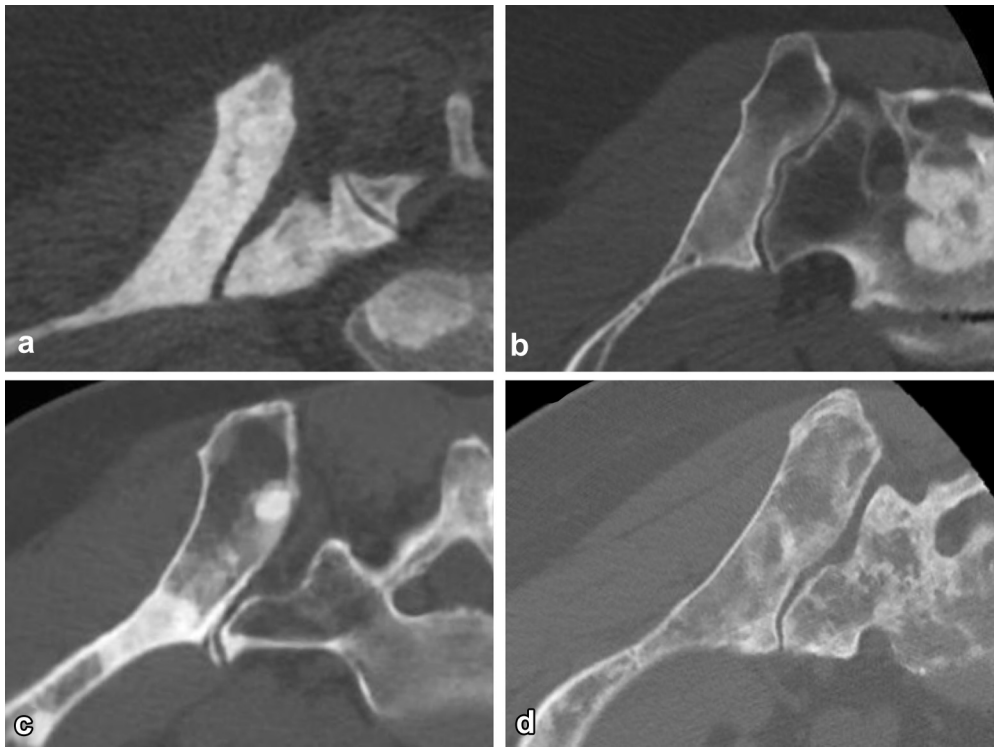

Figure 1. CT images demonstrate different lesion types of metastatic prostate cancer. **(a)** Lesion with predominantly dense sclerosis. **(b)** Lesion with predominantly subtle sclerosis. **(c)** Mixed lesion with areas of dense and subtle sclerosis. **(d)** Lesion with areas of radiolucency.

Table 2. Association between Technical Parameters and Biopsy Success Rates

Parameters	Number of Biopsies	Biopsy Success Rate	Odds Ratio (95% CI)	*P*
Anatomic location				
Ilium	59	75% (44/59)	*	*
Pelvis (nonilium)	13	55% (7/13)	0.36 (0.10–1.30)	.12
Extrapelvis	8	63% (5/8)	0.50 (0.10–2.49)	.40
Biopsy needle				
Jamshidi 11-gauge	29	62% (18/29)	*	*
Bonopty 16-gauge	11	73% (8/11)	1.54 (0.33–7.25)	.58
Arrow OnControl power drill	10	50% (5/10)	0.55 (0.12–2.54)	.45
Bonopty 13-gauge	30	80% (24/30)	2.54 (0.73–8.84)	.14
Location of core sample				
Central	64	64% (41/64)		
Peripheral	16	88% (14/16)	4.71 (0.77–28.91)	.09
Distance cortex to lesion, cm				
$>$ 1.6	33	58% (19/33)		
$\leq$ 1.6	47	77% (36/47)	2.34 (0.86–6.38)	.09
Number of cores				
$\leq$ 2	32	56% (18/32)	*	*
3	17	76% (13/17)	2.43 (0.64–9.28)	.19
4	22	77% (17/22)	2.56 (0.77–8.50)	.12
$\geq$ 5	9	78% (7/9)	3.51 (0.65–18.73)	.14

CI = confidence interval.
*Serves as reference variable for analysis with general estimating equations.

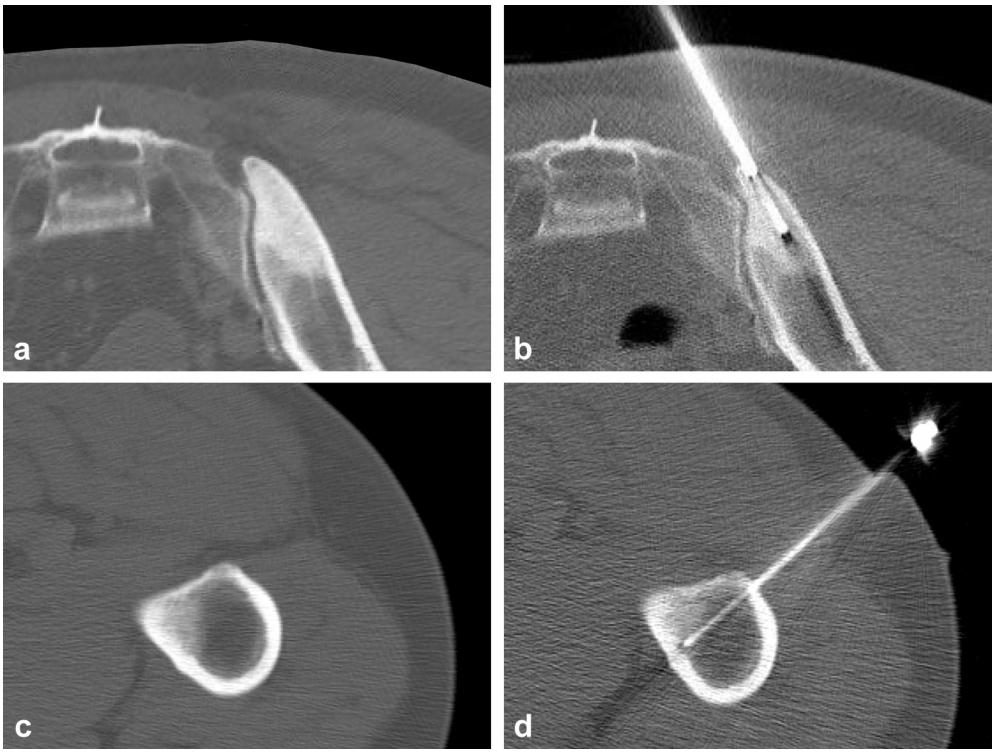

Figure 2. CT–guided needle placement with images showing examples of biopsy site locations within the **(a, b)** central and **(c, d)** peripheral portions of 2 different lesions. Both lesions were positive for tumor cells on histology.

(history of treatment to the pelvis, lumbar spine, or prostate bed < 3 years before biopsy).

Biopsy Procedure

All procedures described in this study were performed by 4 subspecialty-trained musculoskeletal radiologists (E.F., B.B., D.M., T.M.L.; mean experience, 13 y; range, 6–25 y). Biopsy sites were selected based on clinical judgment and safety. Sites of prior external-beam radiation were excluded if possible. All biopsies were performed with image guidance using multidetector CT scanners (Discovery 750HD; GE Healthcare, Chicago, Illinois; Brilliance CT 16 slice–DS; Philips Healthcare, Best, Netherlands). Local anesthesia using 1% lidocaine was administered at the skin surface and along the anticipated tract of the biopsy needle. Conscious sedation was not used during any of the biopsy procedures. Core samples were obtained with a Jamshidi 11-gauge needle (CareFusion Corp, Vernon Hills, Illinois), Bonopty 13-gauge needle (AprioMed, Uppsala, Sweden), Bonopty 16-gauge needle (AprioMed), or Arrow OnControl power drill biopsy set (Teleflex Inc, Morrisville, North Carolina). There were 2–6 cores obtained per biopsy. A cytopathologist was not present for preliminary assessment of the samples during the procedure.

Tissue Processing

Biopsy specimens were processed for histologic evaluation and molecular analysis as previously described (12). Two board-certified genitourinary pathologists (G.V.T., J.H.) reviewed all biopsy specimens for the presence of tumor. Biopsies were considered successful for histologic confirmation if specimens contained $\geq 5\%$ tumor. Unsuccessful biopsies had either no tumor present (ie, normal bone, crush artifact) or insufficient tumor for next-generation sequencing ($< 5\%$ tumor). Specimens were considered positive for successful acquisition of molecular material if the isolated RNA was of sufficient quality for sequencing. Histology was performed in all specimens, whereas RNA analysis was available only in 55 of 80 specimens.

Analysis of Imaging and Technical Parameters

Imaging and technical parameters used during the biopsy were reviewed retrospectively by 1 radiologist from each center (M.G.H., E.F.; 3–10 y of experience) blinded to the pathology results. The imaging findings from each biopsy were interpreted independently but subsequently adjudicated by consensus between the 2 radiologists.

The anatomic location of the biopsies was classified as ilium, pelvis (nonilium), or extrapelvis. The size of the lesion was categorized as < 2 cm, 2–4 cm, or > 4 cm. The number of core samples was divided into the following categories: ≤ 2, 3, 4, or ≥ 5. The location of the sample within the lesion was characterized as either central or peripheral. Peripheral samples were defined as samples obtained within 5 mm from the interface between normal and diseased bone. The lesion type was defined as lesions with predominantly dense sclerosis, lesions with

Table 3. Association between Imaging Features and Biopsy Success Rates

Imaging Features	Number of Biopsies	Biopsy Success Rate	Odds Ratio (95% CI)	*P*
Lesion type				
Dense sclerosis	15	33% (5/15)	*	*
Subtle sclerosis	23	65% (15/23)	3.48 (0.87–13.98)	.08
Mixed lesions	23	74% (17/23)	5.23 (1.26–21.72)	.02
Areas of radiolucency	19	95% (18/19)	33.8 (3.49–327.85)	.002
Qualitative density at biopsy site—mixed lesions				
Dense sclerosis	3	0% (0/3)		
Subtle sclerosis	20	85% (17/20)	12.8 (1.46–∞)	.02†
Mean attenuation at biopsy site, HU				
≤ 475	62	79% (49/62)	7.32 (2.42–22.13)	.0004
> 475	18	33% (6/18)		
Margins				
Well-circumscribed	14	36% (5/14)		
Ill-defined	66	76% (50/66)	5.46 (1.65–18.04)	.005
Interval growth, < 24 mo				
Yes	47	81% (38/47)	5.42 (1.67–17.53)	.005
No	26	42% (11/26)		
Size, cm				
< 2	17	59% (10/17)	*	*
2–4	24	67% (16/24)	2.14 (0.453–8.57)	.28
> 4 cm	39	74% (29/39)	2.30 (0.68–7.74)	.18
Bone scan—active uptake				
Yes	76	68% (52/76)		
No	4	75% (3/4)	1.21 (0.18–8.17)	.85

CI = confidence interval.
*Serves as reference variable for analysis with general estimating equations.
†Exact logistic regression.

predominantly subtle sclerosis, mixed lesions with areas of dense and subtle sclerosis, or lesions with areas of radiolucency (Fig 1a–d).

The quantitative attenuation at the biopsy site was measured in Hounsfield units in a 3 × 10 mm cylindrical region of interest oriented along the course of the needle at the biopsy site. To calculate a mean attenuation, 3 measurements (HU) were obtained. Lesion margins were categorized as either well-circumscribed or ill-defined. A well-circumscribed margin was defined by a sharp, narrow zone of transition, whereas an ill-defined margin was defined by a hazy, wide zone of transition. Variable sampling techniques were used for lesions with ill-defined margins, including targeting the central (53 of 66) and peripheral (13 of 66) portions of the lesion.

Interval lesion growth was assessed by comparing the CT images obtained during the biopsy procedure with available prior CT imaging. Positive interval growth was defined as a > 25% increase in mean diameter of the lesion demonstrated within the previous 24 months. All patients included in the study had a recent technetium-99m methylene diphosphonate bone scan performed < 3 months before the biopsy. The presence of radiotracer uptake at the biopsy site was evaluated. Additional parameters analyzed included type of biopsy needle and distance from the cortex to the lesion edge (in centimeters).

Statistical Analysis

General estimating equations accounting for intrapatient correlations (72 subjects, 80 biopsies) were used to assess whether biopsy outcome (adequate amount of tumor cells) was associated with the predictor variables (described in Technical Parameters, Imaging Review, and Clinical and Laboratory Data). The continuous predictor variables were empirically subdivided into dichotomous categories based on threshold values chosen to provide good sensitivity without losing too many subjects owing to low specificity. All analyses were adjusted for age. $P < .05$ was considered statistically significant. Statistical analysis was performed using STATA version 13 (StataCorp LLC, College Station, Texas).

RESULTS

Overall Success Rate

The technical success rate of CT-guided bone biopsy was 69% (55 of 80) based on histologic cellular confirmation of cancer (≥ 5% tumor). The percent tumor in each specimen was < 5% in 25 cases, 5%–49% in 37 cases, and ≥ 50% in 18 cases. The success rate based on successful isolation of RNA for sequencing within a subset of the population was 64% (35 of 55). The procedures were well tolerated, and no complications were encountered in any of the biopsy procedures.

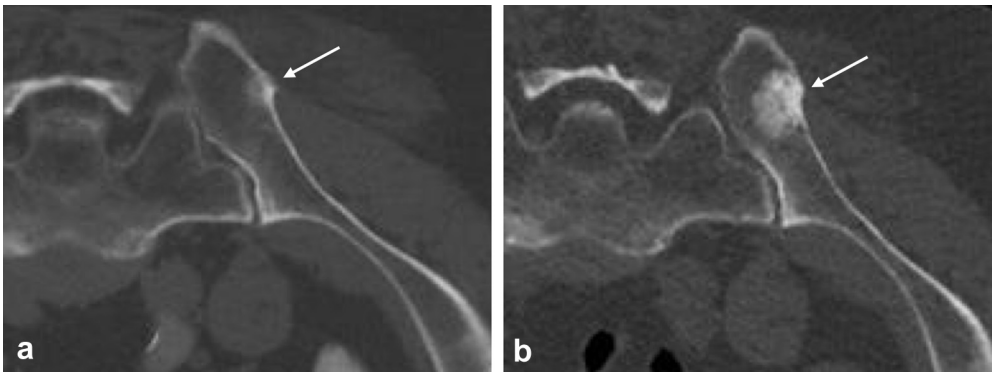

Figure 3. CT images showing evidence of interval growth. Images obtained **(a)** 8 months before biopsy and **(b)** at the time of biopsy demonstrate a > 25% increase in diameter of an osteoblastic lesion in the ilium wing (arrow) compatible with interval growth. The biopsy specimen was positive for tumor cells on histology.

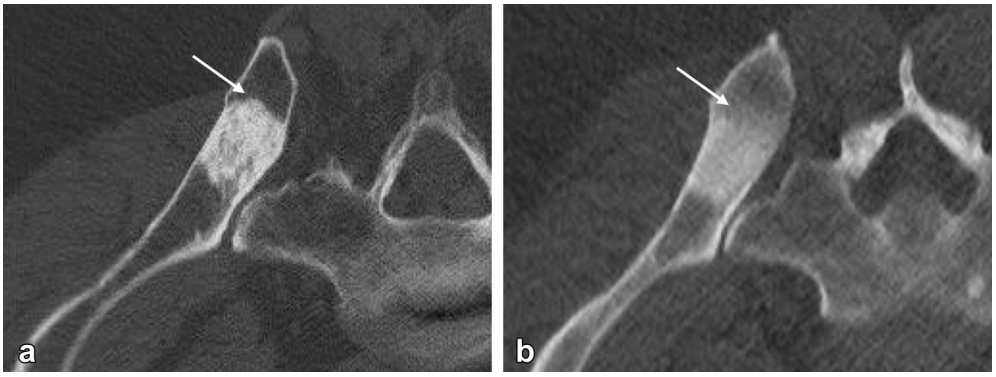

Figure 4. CT images illustrates the 2 different classifications of margins encountered in osteoblastic prostate cancer lesions. **(a)** Well-circumscribed margins with narrow zone of transition (negative). **(b)** Ill-defined margins with infiltrative, wide zone of transition (positive).

Technical Parameters

The average distance from the cortex to the lesion edge along the needle tract was approximately 30% shorter in the successful biopsy group compared with the unsuccessful biopsy group (1.3 cm ± 0.2 vs 1.8 cm ± 0.3; $P = .09$). An empirically determined cutoff value of 1.6 cm resulted in a statistical trend in diagnostic yield (77% [36 of 47] for ≤ 1.6 cm vs 58% [19 of 33] for > 1.6 cm; $P = .09$) (Table 2). There was also a statistical trend with regard to the location of the actual biopsy site within the lesion (Fig 2a–d); a successful biopsy was demonstrated in 88% (14 of 16) of peripheral samples versus 64% (41 of 64) of central samples ($P = .09$). In terms of the number of core samples, the biopsy success rate was 58% (18 of 32) for ≤ 2 specimens, increased to 76% (13 of 17) for 3 specimens ($P = .19$), and plateaued with each additional specimen (4 samples, 77% [17 of 22], ≥ 5 samples, 78% [7 of 9]; $P = .29$).

Imaging Review

Figure 1a–d shows the 4 different types of osteoblastic lesions identified in this study. The lowest biopsy success rate of 33% (5 of 15) (Table 3) was seen in lesions of predominantly dense sclerosis (Fig 1a). In comparison, there was a statistical trend with a higher success rate of 65% (15 of 23) ($P = .08$) in lesions of predominantly subtle sclerosis (Fig 1b) and a statistically significantly higher success rate of 74% (17 of 23) ($P = .02$) in mixed lesions containing areas of both dense and subtle sclerosis (Fig 1c). Given the fact that mixed lesions contain areas of both dense and subtle sclerosis, the diagnostic yield depended on the qualitative density at the biopsy site. If the biopsy specimen was obtained in an area of subtle sclerosis, the success rate was 85% (17 of 20), whereas if the biopsy specimen was obtained in an area of dense sclerosis, the success rate was 0% (0 of 3) ($P = .02$). The highest success rate of 95% (18 of 19) in lesions containing areas of radiolucency (Fig 1d) was statistically significantly higher than both lesions of predominantly dense sclerosis ($P = .002$) and lesions of predominantly subtle sclerosis ($P = .04$). These areas of radiolucency were distinctly lower in attenuation than sclerotic bone but were not traditionally lytic because of the lack of obvious soft tissue or bone destruction. Lesions with areas of radiolucency demonstrated a higher concentration of tumor relative to all other lesion types (28.1% ± 4.8 vs 17.2% ± 2.7; $P = .04$). Similarly, lesions of predominantly subtle sclerosis had a higher proportion

of tumor cellularity compared with lesions of predominantly dense sclerosis (25.2% ± 4.2 vs. 5.3% ± 5.2; $P = .003$).

Successful biopsies were found to have a lower mean attenuation of 330 HU ± 23 compared with 475 HU ± 49 in unsuccessful biopsies ($P = .005$). An empirically determined cutoff value of 475 HU resulted in a statistically significant difference in diagnostic yield (79% [49 of 62] for ≤ 475 HU vs 33% [6 of 18] for > 475 HU; $P = .001$). Lesions with ≤ 475 HU demonstrated a higher proportion of tumor cellularity compared with lesions with > 475 HU (23.8% ± 2.6 vs 6.2% ± 4.8; $P = .001$).

Biopsy success rates were significantly associated with interval growth of the lesion preceding biopsy. Lesions with at least a 25% increase in mean diameter compared with a prior CT scan within the previous 24 months (Fig 3a, b) demonstrated significantly better biopsy outcomes with a success rate of 81% (38 of 47). In contrast, lesions unchanged in size over the same time period were found to have adequate tumor yield in only 42% (11 of 26) of cases ($P = .005$).

Lesions with ill-defined margins were statistically more likely to have a successful biopsy compared with lesions with well-circumscribed margins (76% [50 of 66] vs. 36% [5 of 14]; $P = .005$) (Fig 4a, b). Lesions with ill-defined margins demonstrated a higher proportion of tumor cellularity compared with lesions with well-circumscribed margins (22.2% ± 2.6 vs. 8.6% ± 5.6; $P = .03$).

Clinical and Laboratory Data

Alkaline phosphatase was the only laboratory variable shown to be statistically significantly associated with biopsy outcome (Table 4). As a categorical variable, 83% (34 of 41) of biopsies were successful when alkaline phosphatase was > 110 U/L compared with 50% (18 of 36) of biopsies when alkaline phosphatase was ≤ 110 U/L ($P = .001$). As a numerical variable, the average level of alkaline phosphatase was 246 U/L ± 32 in successful biopsies compared with 125 U/L ± 23 in unsuccessful biopsies ($P = .03$). Although relatively higher levels of lactate dehydrogenase (300 U/L ± 82 vs 237 U/L ± 21; $P = .61$), higher levels of PSA (232 μg/L ± 86 vs 101 μg/L ± 30; $P = .30$), and lower levels of hemoglobin (12.0 g/dL ± 0.2 vs 12.3 g/dL ± 0.3; $P = .49$) were observed in the positive biopsy group, the differences were not statistically significant.

A slightly lower biopsy success rate was observed in men receiving bone-modifying agents (63% [24 of 38] vs 74% [31 of 42]); however, the difference was not statistically significant ($P = .38$). No differences were seen on the basis of the

Table 4. Association between Clinical Variables and Biopsy Success Rates

Variables	Number of Biopsies	Biopsy Success Rate	Odds Ratio (95% CI)	*P*
Alkaline phosphatase, U/L				
> 110	41	83% (34/41)	6.36 (2.14–18.88)	.001
≤ 110	36	50% (18/36)		
PSA, μg/L				
> 82	30	77% (23/30)	1.91 (0.72–5.03)	.19
≤ 82	50	64% (32/50)		
Hemoglobin, g/dL				
≤ 13.4	54	72% (39/54)	1.57 (0.56–4.39)	.39
> 13.4	21	62% (13/21)		
Bone-modifying agent				
Yes	38	63% (24/38)		
No	42	74% (31/42)	1.56 (0.58–4.20)	.38
Type of bone-modifying agent				
Zoledronate	8	63% (5/8)	0.82 (0.14–4.81)	.83
Denosumab	30	63% (19/30)		
Bone-modifying agent—treatment length				
≤ 12 mo	18	61% (11/18)		
> 12 mo	20	65% (13/20)	1.75 (0.38–7.99)	.47
External-beam radiation*				
Yes	20	60% (12/20)		
No	56	71% (40/56)	1.73 (0.58–5.20)	.33
Systemic chemo-/immunotherapy†				
Yes	10	80% (8/10)	2.34 (0.42–13.21)	.34
No	30	57% (17/30)		

CI = confidence interval; PSA = prostate-specific antigen.
*Subset of population (n = 76).
†Subset of population (n = 40).

type of bone-modifying agent (63% [5 of 8] for zoledronate vs 63% [19 of 30] for denosumab; $P = .83$) or the length of therapy (61% [11 of 18] for $\leq$ 12 months vs 65% [13 of 20] for $>$ 12 months; $P = .47$). Biopsy success rates were also slightly lower in patients who received external-beam radiation (60% [12 of 20] vs 71% [40 of 56]), but the differences were not statistically significant ($P = .33$).

DISCUSSION

In this study, most CT-guided bone tumor biopsies yielded material suitable for histologic and molecular analyses in patients with mCRPC. Radiologic characteristics associated with success included osteoblastic metastases with areas of radiolucency or minimal low-attenuation sclerosis, lesions with ill-defined margins, and lesions with recent interval growth. Additional parameters, such as elevated serum alkaline phosphatase, sampling from the periphery of lesions, and selecting lesions closest to the cortex, also resulted in improved biopsy outcomes.

The number of prior studies specifically examining CT-guided bone biopsies in men with mCRPC has been limited, and in contrast to the present study, far fewer variables were analyzed. Spritzer et al (12) analyzed 54 biopsies and found a 67% success rate based on histologic confirmation of tumor cells and a 40% success rate based on successful RNA isolation. In a smaller, more limited study of 30 biopsies, McKay et al (10) reported a 77% success rate based only on histologic confirmation. In regard to adequate material for histologic determination, the success rates in the present study were very similar to these 2 studies; however, the diagnostic yield of the present study based on successful isolation of RNA for sequencing was markedly higher than that of Spritzer et al. Given that the methods for tissue processing and RNA isolation were similar, a good explanation for the differences is not available. However, success rates improved in later biopsies likely as a result of more precise technique and experience.

The historically low biopsy success rates of osteoblastic lesions compared with other osseous lesions have often been attributed to the tightly packed sclerotic matrix resulting in limited growth and decreased cellularity (6). However, studies have shown a significant degree of heterogeneity and variability in the histologic makeup of osteoblastic lesions. Reports based on postmortem analyses have described 5 different histologic patterns of prostate cancer tumor metastases in bone with variable proportion of tumor volume ranging from $<$ 5% in osteodense lesions to 88% in osteopenic lesions (2,14). In the present study, lesions of predominantly dense sclerosis demonstrated an average tumor concentration of 4%, corresponding with a very low 33% biopsy success rate. In contrast, lesions with areas of radiolucency demonstrated an average tumor concentration of 28% and consequently a much higher 95% biopsy success rate. Although both of these biopsy success rates fall far outside of the range of diagnostic yields (54%–77%), which have been reported in the past for "sclerotic lesions" (7–10,12), these results indicate that osteoblastic metastases in mCRPC are not a homogeneous group of lesions. Therefore, the following imaging characteristics suggestive of increased cellularity can be helpful for improving biopsy tumor yields: lesions with areas of radiolucency, qualitatively subtle sclerosis, mean attenuation $<$ 475 HU, and ill-defined margins.

Radiographic and clinical signs of disease progression are important factors to consider when optimizing tissue yield in patients with mCRPC. In breast cancer metastases, an increase in lesion size has been described as a reliable indicator of the presence of tumor, particularly in osteoblastic lesions where evaluation is often complicated by treatment-related sclerosis (15). The results of the present study suggest a similar relationship in which an increase in lesion size significantly correlates with increased diagnostic yields. Clinically, markers of disease burden, such as hemoglobin, alkaline phosphatase, and PSA, have been reported to correlate with outcomes in blind bone marrow biopsies in patients with mCRPC (11,16). In the present study, only alkaline phosphatase was found to be associated with tumor yield. However, this finding may indicate a lesser degree of specificity of PSA and hemoglobin in patients with mCRPC. For example, anemia may occur as a consequence of marrow infiltration but can also be caused by a number of different factors, including androgen deprivation therapy or other anticancer therapies (17). Alkaline phosphatase has been shown to be more specific for bone turnover and tumor growth (18).

This study has limitations mainly as a consequence of the study design. There was some degree of selection bias. Lesions were primarily selected for biopsy on the basis of feasibility and safety rather than true randomization. Biopsy techniques were variable depending on the performing radiologist, the type of needle, and the number of core samples obtained. A degree of interobserver variability is always a consideration in a study based on image interpretation. However, in this analysis, the imaging was reviewed, analyzed, and adjudicated by consensus between the same 2 radiologists.

In conclusion, CT–guided bone tumor biopsies can be successfully used for acquisition of cellular and molecular material for analyses in patients with osteoblastic prostate cancer metastases. Given the increasing number of biopsies performed for personalized management in patients with mCRPC, careful consideration of procedural techniques, prior imaging, and certain clinical factors can significantly increase diagnostic yield in bone tumor biopsies. The most important radiologic criteria associated with a higher success rate are lesions with areas of radiolucency or minimal low-attenuation sclerosis, lesions with ill-defined margins, and lesions with recent interval growth.

ACKNOWLEDGMENTS

This study was supported by a Stand Up To Cancer (SU2C) Dream Team award (SU2C-AACR-DT0812); this research

grant is administered by the American Association for Cancer Research, the scientific partner of SU2C. Additional funding was received from a Department of Defense Synergistic Idea Award (W81XWH-13-1-0420).

REFERENCES

1. Howlader N, Noone AM, Krapcho M, et al., editors. *SEER Cancer Statistics Review, 1975-2013*. Bethesda, MD: National Cancer Institute; 2015.
2. Roudier MP, True LD, Higano CS, et al. Phenotypic heterogeneity of end-stage prostate carcinoma metastatic to bone. Hum Pathol 2003; 34:646–653.
3. Shah RB, Mehra R, Chinnaiyan AM, et al. Androgen-independent prostate cancer is a heterogeneous group of diseases: lessons from a rapid autopsy program. Cancer Res 2004; 64:9209–9216.
4. Feldman BJ, Feldman D. The development of androgen-independent prostate cancer. Nat Rev Cancer 2001; 1:34–45.
5. Harris WP, Mostaghel EA, Nelson PS, Montgomery B. Androgen deprivation therapy: progress in understanding mechanisms of resistance and optimizing androgen depletion. Nat Clin Pract Urol 2009; 6:76–85.
6. Hensel J, Thalmann GN. Biology of bone metastases in prostate cancer. Urology 2016; 92:6–13.
7. Fraser-Hill MA, Renfrew DL. Percutaneous needle biopsy of musculoskeletal lesions. 1. Effective accuracy and diagnostic utility. AJR Am J Roentgenol 1992; 158:809–812.
8. Wu JS, Goldsmith JD, Horwich PJ, Shetty SK, Hochman MG. Bone and soft-tissue lesions: what factors affect diagnostic yield of image-guided core-needle biopsy? Radiology 2008; 248:962–970.
9. Vieillard MH, Boutry N, Chastanet P, Duquesnoy B, Cotten A, Cortet B. Contribution of percutaneous biopsy to the definite diagnosis in patients with suspected bone tumor. Joint Bone Spine 2005; 72:53–60.
10. McKay RR, Zukotynski KA, Werner L, et al. Imaging, procedural and clinical variables associated with tumor yield on bone biopsy in metastatic castration-resistant prostate cancer. Prostate Cancer Prostatic Dis 2014; 17:325–331.
11. Ross RW, Halabi S, Ou SS, et al. Predictors of prostate cancer tissue acquisition by an undirected core bone marrow biopsy in metastatic castration-resistant prostate cancer—a Cancer and Leukemia Group B study. Clin Cancer Res 2005; 11:8109–8113.
12. Spritzer CE, Afonso PD, Vinson EN, et al. Bone marrow biopsy: RNA isolation with expression profiling in men with metastatic castration-resistant prostate cancer—factors affecting diagnostic success. Radiology 2013; 269:816–823.
13. Eisenhauer EA, Therasse P, Bogaerts J, et al. New response evaluation criteria in solid tumours: revised RECIST guideline (version 1.1). Eur J Cancer 2009; 45:228–247.
14. Roudier MP, Morrissey C, True LD, Higano CS, Vessella RL, Ott SM. Histopathological assessment of prostate cancer bone osteoblastic metastases. J Urol 2008; 180:1154–1160.
15. Hamaoka T, Madewell JE, Podoloff DA, Hortobagyi GN, Ueno NT. Bone imaging in metastatic breast cancer. J Clin Oncol 2004; 22:2942–2953.
16. Lorente D, Omlin A, Zafeiriou Z, et al. Castration-resistant prostate cancer tissue acquisition from bone metastases for molecular analyses. Clin Genitourin Cancer 2016; 14:485–493.
17. Nalesnik JG, Mysliwiec AG, Canby-Hagino E. Anemia in men with advanced prostate cancer: incidence, etiology, and treatment. Rev Urol 2004; 6:1–4.
18. Garnero P. Markers of bone turnover in prostate cancer. Cancer Treat Rev 2001; 27:187–192; discussion 193–1966.

APPENDIX A.

Disease progression was defined as (*i*) a minimum PSA level of 2 ng/mL that had risen on at least 2 separate measurements at least 1 week apart, (*ii*) progression on bone scintigraphy (> 2 new lesions), (*iii*) soft tissue progression according to Response Evaluation Criteria In Solid Tumors (13), or (*iv*) symptomatic progression in an area of radiographically evident disease.